

31310 LINEAR CONTROL DESIGN 2

COMPULSORY ASSIGNMENT 2015 : LOUDSPEAKER CONTROL

by

KATLEEN BLANCHET s150798

TITOUAN BOULMIER s150810

$$f(x+\Delta x) = \sum_{i=0}^{\infty} \frac{(\Delta x)^i}{i!} f^{(i)}(x)$$

$\Delta \int_a^b \Theta^{\sqrt{17}} + \Omega \int \delta e^{in} = -1$

$\infty = \{2.7182818284\}^{\circ}$

$\chi^2, \sum, \approx, \lambda$

$!$

December 3, 2015



Technical University of Denmark
Department of Electrical Engineering

Contents

1	Distortion Attenuation for Loudspeakers	1
1.1	Moving-coil Loudspeakers	1
1.1.1	Loudspeakers electrical equivalent circuit	1
	Problem 1	2
	Problem 2	2
	Problem 3	3
1.1.2	Harmonic Distortion	4
	Problem 4	4
	Problem 5	5
1.1.3	Linearised Model	6
	Problem 6	6
	Problem 7	8
	Problem 8	9
	Problem 9	10
1.1.4	Harmonic distortion and fictitious disturbances	11
	Problem 10	11
	Problem 11	12
1.2	Distortion Attenuation	13
1.2.1	System discretization	13
	Problem 12	13
	Problem 13	13
1.2.2	Voice coil position reference tracking	15
	Problem 14	15
	Problem 15	15
	Problem 16	17
	Problem 17	18
	Problem 18	20
1.2.3	Output feedback voice coil position tracking control with disturbance rejection	21
	Problem 19	21

Problem 20	22
Problem 21	23
Problem 22	23
A SIMULINK Model of the Nonlinear System	24
B Block Diagram of the Linearised Loudspeaker	25
C SIMULINK Model of the Linear System	26
D SIMULINK Model of the Linear System with Disturbance in Continuous Time	27
E SIMULINK Model of the Linear System with Disturbance in Discrete Time	28
F SIMULINK Model of the Discrete Time Linear System with the Feedback Controller	29
G SIMULINK Model of the Continuous Time Linear System with the Discrete Time Feedback	30
H SIMULINK Model of the Nonlinear Model with the Discrete Time Feedback	31
I SIMULINK Model of Kalman filter for the linear model with disturbance	32

Exercice 1

Distortion Attenuation for Loudspeakers

1.1 Moving-coil Loudspeakers

1.1.1 Loudspeakers electrical equivalent circuit

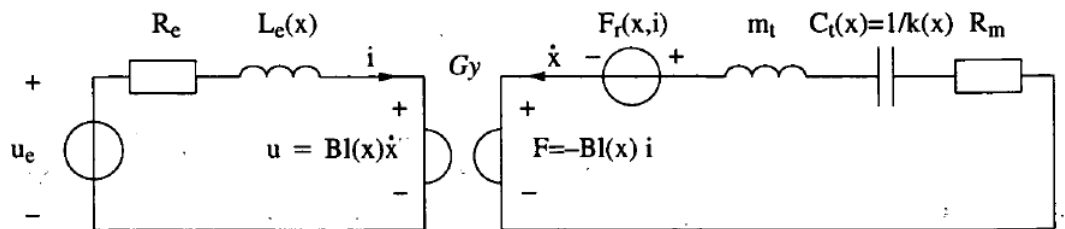


Figure 1.1: Electrical equivalent lumped element model of the voltage driven electrodynamic loudspeaker for low frequencies. The coupling between the electrical and mechanical domain is performed through the gyrator with gyration constant $Bl(x)$.

$$u_e = R_e i + \frac{dL_e(x)}{dx} \frac{dx}{dt} i + L_e(x) \frac{di}{dt} + Bl(x) \frac{dx}{dt} \quad (1.1)$$

$$Bl(x)i = m_t \frac{d^2x}{dt^2} + R_m \frac{dx}{dt} + k(x)x - \frac{1}{2} \frac{dL_e(x)}{dx} i^2 \quad (1.2)$$

where

$$Bl(x) = Bl_0 + b_1x + b_2x^2 \quad (1.3)$$

$$L_e(x) = L_{e0} + l_1x + l_2x^2 \quad (1.4)$$

$$k(x) = k_0 + k_1x + k_2x^2 \quad (1.5)$$

Problem 1

By means of Eqs (1.1), (1.2), (1.3), (1.4) and (1.5), we can identify 3 state variables x , \dot{x} and i . We can also identify the input u_e .

$$\mathbf{x} = \begin{pmatrix} x \\ \dot{x} \\ i \end{pmatrix} \text{ and } \mathbf{u} = (u_e)$$

Then, we can derive the nonlinear dynamical state space model to obtain

$$\dot{x} = \dot{x} \quad (1.6)$$

$$\ddot{x} = \frac{(Bl_0 + b_1x + b_2x^2)i - R_m\dot{x} - (k_0 + k_1x + k_2x^2)x + \frac{1}{2}(l_1 + 2l_2x)\dot{x}^2}{m_t} \quad (1.7)$$

$$\dot{i} = \frac{u_e - (R_e + (l_1 + 2l_2x)\dot{x}^2)i - (Bl_0 + b_1x + b_2x^2)\dot{x}}{L_{e0} + l_1x + l_2x^2} \quad (1.8)$$

In matrix format, we have

$$\dot{\mathbf{x}} = f(\mathbf{x}) + g(\mathbf{x})\mathbf{u} \quad (1.9)$$

with

$$f(\mathbf{x}) = \begin{pmatrix} \dot{x} \\ \ddot{x} \\ \dot{i} \end{pmatrix} = \begin{pmatrix} \dot{x} \\ \frac{(Bl_0 + b_1x(1) + b_2x(1)^2)x(3) - R_mx(2) - (k_0 + k_1x(1) + k_2x(1)^2)x(1) + \frac{1}{2}(l_1 + 2l_2x(1))x(2)x(3)^2}{m_t} \\ \frac{-(R_e + (l_1 + 2l_2x(1))x(2)^2)x(3) - (Bl_0 + b_1x(1) + b_2x(1)^2)x(2)}{L_{e0} + l_1x(1) + l_2x(1)^2} \end{pmatrix} \quad (1.10)$$

$$g(\mathbf{x}) = \begin{pmatrix} 0 \\ 0 \\ \frac{1}{L_{e0} + l_1x(1) + l_2x(1)^2} \end{pmatrix} \quad (1.11)$$

Problem 2

The block diagram of the nonlinear model figure A.1 in Appendix A shows how the electrical and the mechanical subsystems are interconnected. This block diagram is also our SIMULINK model. The system is quickly stabilised (around 1 s) but as we are going to analyse it in the frequency domain, a longer period of time will provide better results. Thus, the TIME_SIM is set to 5 s.

Problem 3

The input voltage is set to $u_e = A_u \sin(2\pi f_c t)$, where $A_u = 5 \text{ V}$ and $f_c = 20 \text{ Hz}$. Then the nonlinear system implemented in P2 is simulated to get the states responses. For more clarity, the time domain responses were plotted from 0 to 2s. Moreover, the system is not stabilised at the beginning of the simulation, so it was decided to remove the first second for the spectral analysis. To visualise the signals in the frequency domain, we used the *power_spectral_density* function given in the assignment [1] with $F_s = \frac{1}{\text{TIME_SIM}} = 10 \text{ kHz}$. The function output gives the power spectral density P_{xx} in [$\text{Amplitude}^2/\text{Hz}$]. In order to convert it in [dB/Hz], we use:

$$P_{dB} = 10 \log_{10}(P_{xx})$$

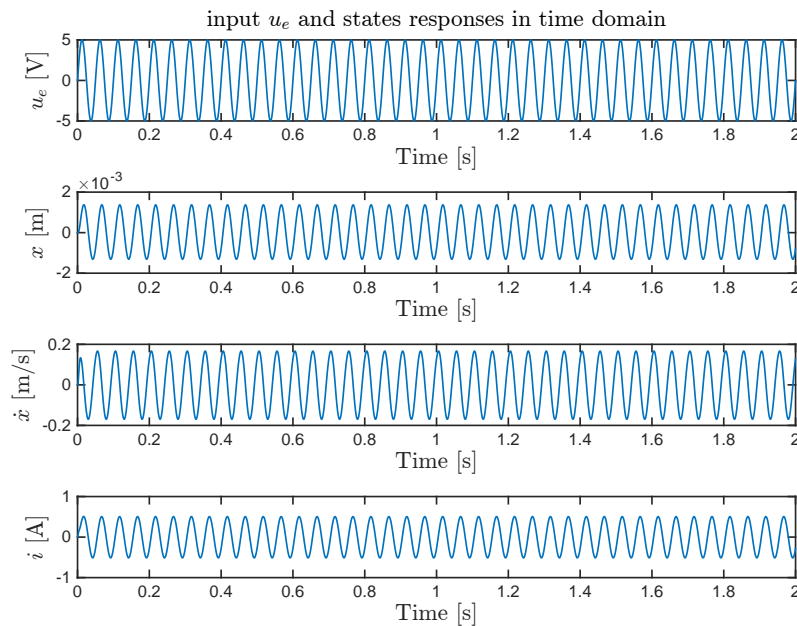


Figure 1.2: Nonlinear Model: input u_e and the states responses in the time domain

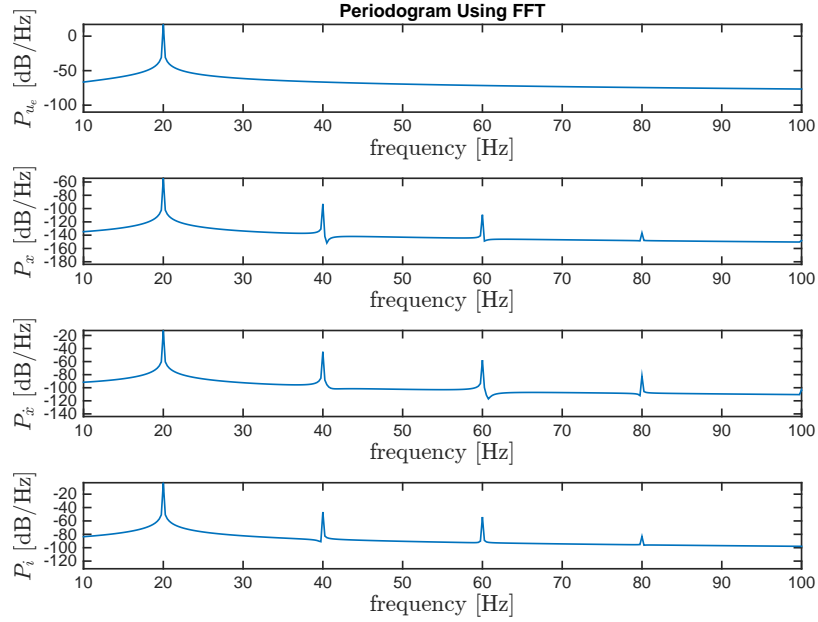


Figure 1.3: Nonlinear Model: input u_e and the states responses in the frequency domain

In the time domain (see figure 1.2), we notice that the states responses are sinusoidal, with constant amplitudes. The system looks stable. Moreover, the frequency of the states seems similar to the frequency of the input signal, with slight variations. The explanation for these changes is given in the frequency domain, figure 1.3, where we can see several more spikes at the frequencies $f_n = n f_c$, smaller than the fundamental one at $f_c = 20 \text{ Hz}$. The presence of other harmonics in the states responses, which are not in the input, shows the effects of the nonlinearity of the system. It may be due to the fact that the voice coil displacement is limited: when it goes too far, the spider prevents it from leaving the magnetic field, which can cause the harmonic distortion.

1.1.2 Harmonic Distortion

We are now going to study the harmonic distortion observed in the states responses in the frequency domain.

Problem 4

The analysis will be restricted to the voice coil velocity \dot{x} . The Total Harmonic Distortion (THD) is described by

$$THD = \frac{\sqrt{\sum_{n=2}^N A_n^2}}{\sqrt{\sum_{n=1}^N A_n^2}} \cdot 100\% \quad (1.12)$$

where A_1 the amplitude of the fundamental frequency and A_n the amplitudes of the harmonics.

To compute THD for the 5 harmonics after the fundamental frequency f_c we need to find the 6 amplitudes corresponding to the fundamental frequency pikes and the 5 following harmonics. To that purpose, a function *amplitude* was implemented (see below) with x the signal and fr the frequency at which we desire to know the amplitude of the spike. The Fast Fourier Transform is computed but not the spectral power density as previously.

```
function [ res ] = amplitude(x, TIME_SIM, fr)
    NFFT = length(x);
    X = fft(x,NFFT) / (NFFT);
    X = 2*abs(X(1:NFFT/2+1));
    res = X(fr*TIME_SIM+1);
end
```

Finally for a $TIME_SIM = 5s$, $THD_x = 2.435\%$. We then use the equations (1.13) and (1.14) to compute the second and third order harmonic distortion. We obtain $d_2 = 2.37\%$ and $d_3 = 0.54\%$.

$$d_2 = \frac{A_2}{\sqrt{A_1^2 + A_2^2}} \cdot 100\% \quad (1.13)$$

$$d_3 = \frac{A_3}{\sqrt{A_1^2 + A_3^2}} \cdot 100\% \quad (1.14)$$

We can notice that d_2 corresponds to the THD calculated for $N = 2$. Because the amplitudes of the harmonics decrease when the order gets bigger, it is logical that the values of THD and d_2 are quite similar. On the contrary, A_3 is negligible in front of A_1 , that is why d_3 is small compare to the THD.

Problem 5

In order to study the effect of the variations of the frequency f_c and the amplitude A_u of the input u_e on the second and third order harmonic distortions, we have computed d_2 and d_3 for a range of A_u and f_c . The results can be seen on the figure 1.4. According to the graphic, the variations of the amplitude of the input do not affect the shape of the distortion levels. The amplitude has only an impact on the value of the distortion from 20 to 60 Hz. If it doubles, the pourcentage of the distortion will also be multiplied by two. On the other hand, when the fundamental frequency increases, the distortion levels

d_2 and d_3 are stabilising at low values, nearly 0% for d_3 . It can be explained by the fact that the more the fundamental frequency grows, the more the harmonic pikes will be far from it as they correspond to nf_c . Their amplitude will be affected and will become of minor importance in front of the amplitude of the fundamental pike.

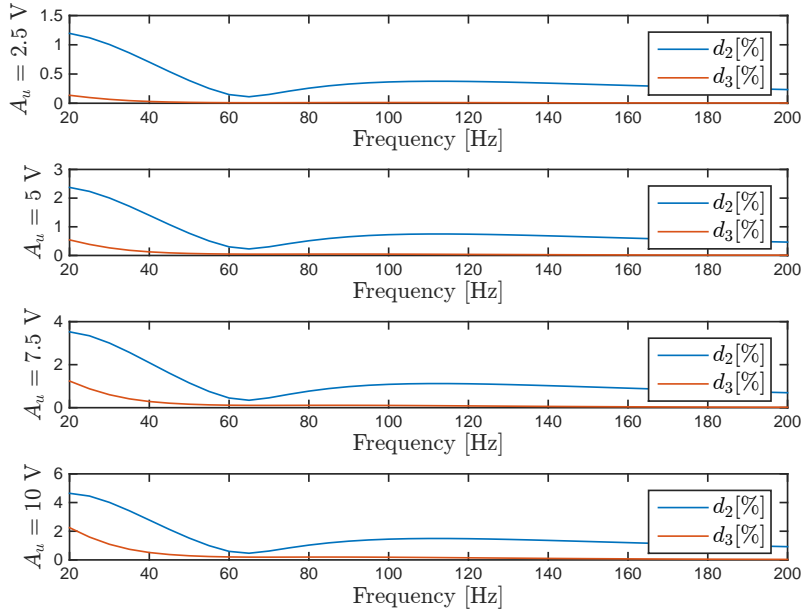


Figure 1.4: Effect of the variations of the frequency f_c and the amplitude A_u of the input u_e on the second and third order harmonic distortions

1.1.3 Linearised Model

The measured output is set to the voice coil current. Therefore $y(t) = r(x) = i(t)$. We also take $u_e = 0$ for the analysis of the linear and nonlinear model around the resting position of the voice coil.

Problem 6

All time derivatives are set to zero in order to determine the stationary states. Therefore, we have $\frac{dx}{dt} = 0$ and equations (1.1) and (1.2) are rewritten below:

$$u_e = R_e i \quad (1.15)$$

$$Bl(x)i = k(x)x \quad (1.16)$$

As $u_e = 0$, from (1.15) we obtain $i = 0$ and we deduce by substituting in (1.16) that $k(x)x = 0$. Then $k(x) = 0$ or $x = 0$. The discriminant of the polynomial $k(x)$ of degree 2 is $\Delta = k_1^2 - 4k_2k_0 < 0$. The voice coil displacement x being real, we discard this value and

get:

$$\mathbf{x}_0 = \begin{pmatrix} 0 \\ 0 \\ 0 \end{pmatrix}$$

We linearise the model $\dot{\mathbf{x}} = h(\mathbf{x}, \mathbf{u})$ with $h(\mathbf{x}) = f(\mathbf{x}) + g(\mathbf{x})\mathbf{u}$ around the stationary states:

$$x(t) = x_0 + \Delta x(t) = \Delta x(t)$$

$$\dot{x}(t) = \dot{x}_0 + \Delta \dot{x}(t) = \Delta \dot{x}(t)$$

$$i(t) = i_0 + \Delta i(t) = \Delta i(t)$$

The linear model can then be written in the form:

$$\dot{\mathbf{x}} = A\mathbf{x} + B\mathbf{u}$$

$$y = C\mathbf{x}$$

where

$$A = \begin{pmatrix} \frac{\partial h_1}{\partial x_1} & \frac{\partial h_1}{\partial x_2} & \frac{\partial h_1}{\partial x_3} \\ \frac{\partial h_2}{\partial x_1} & \frac{\partial h_2}{\partial x_2} & \frac{\partial h_2}{\partial x_3} \\ \frac{\partial h_3}{\partial x_1} & \frac{\partial h_3}{\partial x_2} & \frac{\partial h_3}{\partial x_3} \end{pmatrix}_{x_0} \quad B = \begin{pmatrix} \frac{\partial h_1}{\partial u} \\ \frac{\partial h_2}{\partial u} \\ \frac{\partial h_3}{\partial u} \end{pmatrix}_{x_0} \quad C = \begin{pmatrix} \frac{\partial r}{\partial x_1} & \frac{\partial r}{\partial x_2} & \frac{\partial r}{\partial x_3} \end{pmatrix}_{x_0}$$

We obtain:

$$\frac{\partial h_1}{\partial x_1} = 0 \quad \frac{\partial h_1}{\partial x_2} = 1 \quad \frac{\partial h_1}{\partial x_3} = 0$$

$$\frac{\partial h_2}{\partial x_1} = \frac{b_1 x_{30} + 2b_2 x_{10} x_{30} - (k_0 + 2k_1 x_{10} + 3k_2 x_{10}^2) + l_2 x_{20} x_{30}^2}{m_t}$$

$$\frac{\partial h_2}{\partial x_2} = \frac{-R_m + \frac{1}{2} \times (l_1 + 2l_2 x_{10}) x_{30}^2}{m_t}$$

$$\frac{\partial h_2}{\partial x_3} = \frac{Bl_0 + b_1 x_{10} + b_2 x_{10}^2 + (l_1 + 2l_2 x_{10}) x_{20} x_{30}}{m_t}$$

$$\begin{aligned} \frac{\partial h_3}{\partial x_1} &= \frac{(-2l_2 x_{20}^2 x_{30} - (b_1 + 2b_2 x_{10}) x_{20}) \times (L_{e0} + l_1 x_{10} + l_2 x_{10}^2)}{(L_{e0} + l_1 x_{10} + l_2 x_{10}^2)^2} - (l_1 + 2l_2 x_{10}) \times \\ &\quad \frac{(-(R_e + (l_1 + 2l_2 x_{10}) x_{20}^2) x_{30} - (Bl_0 + b_1 x_{10} + b_2 x_{10}^2) x_{20})}{(L_{e0} + l_1 x_{10} + l_2 x_{10}^2)^2} \end{aligned}$$

$$\frac{\partial h_3}{\partial x_2} = -\frac{2(l_1 + 2l_2x_{10})x_{20}x_{30} + Bl_0 + b_1x_{10} + b_2x_{10}^2}{L_{e0} + l_1x_{10} + l_2x_{10}^2}$$

$$\frac{\partial h_3}{\partial x_3} = -\frac{(l_1 + 2l_2x_{10})x_{20}^2 + R_e}{L_{e0} + l_1x_{10} + l_2x_{10}^2}$$

$$\frac{\partial h_1}{\partial u} = 0 \quad \frac{\partial h_2}{\partial u} = 0 \quad \frac{\partial h_3}{\partial u} = \frac{1}{L_{e0} + l_1x_{10} + l_2x_{10}^2}$$

$$\frac{\partial r}{\partial x_1} = 0 \quad \frac{\partial r}{\partial x_2} = 0 \quad \frac{\partial r}{\partial x_3} = 1$$

We then substitute $x_{10} = x_{20} = x_{30} = 0$. Finally, we get:

$$A = \begin{pmatrix} 0 & 1 & 0 \\ -\frac{k_0}{m_t} & -\frac{R_m}{m_t} & \frac{Bl_0}{m_t} \\ 0 & -\frac{Bl_0}{L_{e0}} & -\frac{R_e}{L_{e0}} \end{pmatrix} \quad B = \begin{pmatrix} 0 \\ 0 \\ \frac{1}{L_{e0}} \end{pmatrix} \quad C = \begin{pmatrix} 0 & 0 & 1 \end{pmatrix}$$

Numerically

$$A = \begin{pmatrix} 0 & 1 & 0 \\ -1.20 \cdot 10^5 & -50.46 & 279.19 \\ 0 & -2.57 \cdot 10^3 & -1.40 \cdot 10^3 \end{pmatrix} \quad B = \begin{pmatrix} 0 \\ 0 \\ 177 \end{pmatrix} \quad C = \begin{pmatrix} 0 & 0 & 1 \end{pmatrix} \quad (1.17)$$

We can check these results with the matlab function *linmod(model,x0,u_e)*:

```
[A, B, C, D] = linmod('nonLinearModel', [0; 0; 0], 0);
```

Problem 7

In this problem, we draw the block diagram of the linearised loudspeaker (see figure B.1 in Appendix B) showing the couplings between the different states.

By means of this block diagram, we can make preliminary assessments of the system. Indeed, we can see that the state i seems to be controllable and observable as it is connected to the input u_e and to the output. However, the states x and \dot{x} seem to be controllable as they are also connected to the input u_e but not observable because they are not connected to any output. Moreover the 3 states seem to be stable because of the 2 back-loops.

We can verify our assumptions regarding the controllability and the observability by calculating the *rank* of M_c and M_o .

```

MC = [B A*B A^2*B];
rank(MC) % = 3 controllable
MO=[C
     C*A
     C*A^2];
rank(MO) % = 3 observable
    
```

Problem 8

We can derive analytically the eigenvalues of the system dynamical matrix A .

$$\det(\lambda I - A) = \det \begin{pmatrix} \lambda & -1 & 0 \\ \frac{k_0}{m_t} & \lambda + \frac{R_m}{m_t} & -\frac{Bl_0}{m_t} \\ 0 & \frac{Bl_0}{Le_0} & \lambda + \frac{Re}{Le_0} \end{pmatrix} \quad (1.18)$$

$$= \lambda^3 + \left(\frac{Re}{Le_0} + \frac{Rm}{m_t} \right) \lambda^2 + \left(\frac{RmRe + Bl_0^2}{m_t Le_0} + \frac{k_0}{m_t} \right) \lambda + \frac{k_0 Re}{m_t Le_0} \quad (1.19)$$

We therefore have a third-order polynomial which can be solved with MATLAB but the eigenvalues can also be calculated using

```
lambda = eig(A);
```

Thus, we obtain

$$\lambda = 1,0.10^2 \begin{pmatrix} -2.9573 \\ -5.7648 + 4.8571i \\ -5.7648 - 4.8571i \end{pmatrix} \quad (1.20)$$

We can notice that

$$Re(\lambda_i) < 0, i = 1, 2, 3 \quad (1.21)$$

which means that the system is asymptotically stable. Moreover, using Euler decomposition, the eigenmodes of the system are $e^{\lambda_1 t}$, $e^{\Re(\lambda_2)t} (\cos(\Im(\lambda_2)t) + \sin(\Im(\lambda_2)t))$ and $e^{\Re(\lambda_3)t} (\cos(\Im(\lambda_3)t) - \sin(\Im(\lambda_3)t))$. We can notice that

$$\frac{1}{\lambda_1} = \tau_1 > \tau_2, \tau_3, \quad \text{with } \tau_i = \frac{1}{\sqrt{\Re(\lambda_i)^2 + \Im(\lambda_i)^2}}, \quad i = 2, 3$$

which means that the response of the state x to an input u_e will be slower than the one of i and \dot{x} . We can also see that as λ_2 and λ_3 have an imaginary part which means that the eigenmodes associated to λ_2 and λ_3 will have an oscillatory behavior.

Problem 9

Using the results of Problem 6 (1.17), we can implement a SIMULINK model (see figure C.1 in Appendix C) of the linear system.

Then, we can simulate the linearised model with an input $u_e = A_u \sin(2\pi f_c t)$, where $A_u = 5V$ and $f_c = 20Hz$. The states response in the time domain is plotted figure 1.5 and the PSD is plotted figure 1.6.

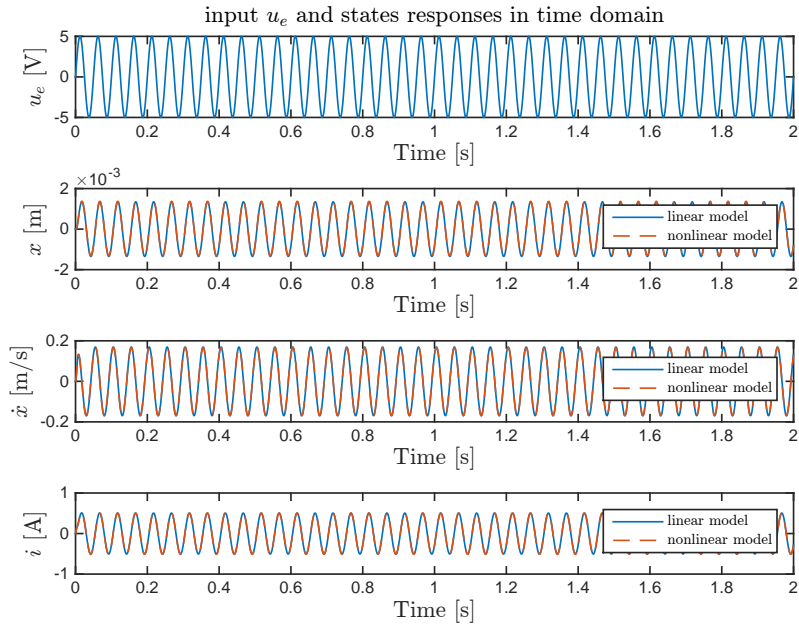


Figure 1.5: u_e and states response to u_e in time domain

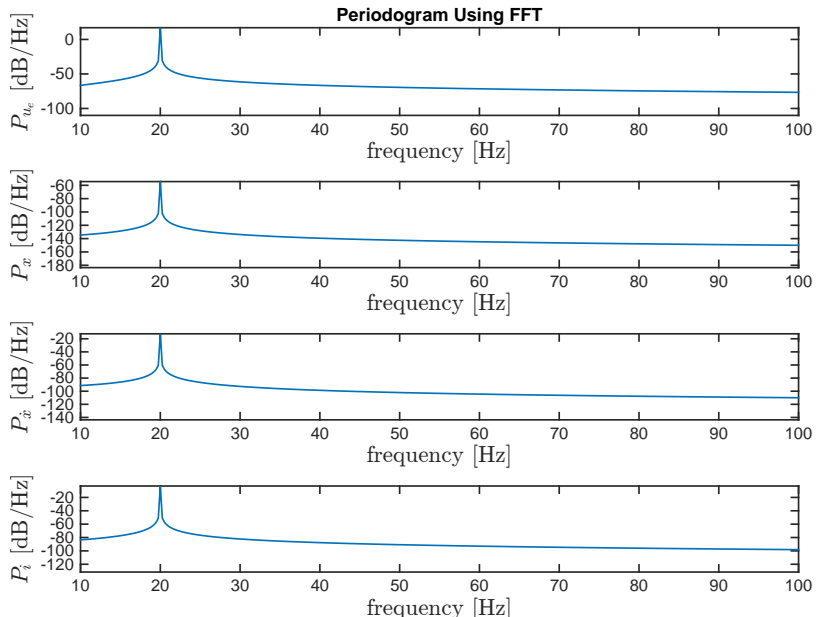


Figure 1.6: PSD of u_e and states

First, comparing the response to the input u_e from the nonlinear model with the linear model in the time domain (figure 1.2), the states response is almost exactly the same, but comparing the PSD of the states response (figure 1.3 and figure 1.6), we can see that the states response is not the same. Indeed, the linearised system is not affected by the harmonic distortion, there is only one frequency present in the states response, the one of $20Hz$ (which has the same magnitude). This result was expected because the nonlinear distortion only affects non-linear systems. Moreover, we have linearised the system with an input $u_e = 0$ which means that we have a linearised system without harmonic, and then, we used a new input u_e with a frequency $f_c = 20Hz$, which means we only obtain a state response with an harmonic of a frequency of f_c .

1.1.4 Harmonic distortion and fictitious disturbances

In this section, we basically want to add a disturbance in order to obtain the same output with the linearised system than with the nonlinear system (the analysis is restrained to the second and third order harmonics). Thus, the output $i(t)$ should be

$$y_{nl}(t) = A_1 \sin(2\pi f_c t + \psi_1) + A_2 \sin(4\pi f_c t + \psi_2) + A_3 \sin(6\pi f_c t + \psi_3) \quad (1.22)$$

Problem 10

First, we extend our model with two input disturbances such that the linear output will also show the second and third order harmonics. The new linearised model is

$$\begin{aligned} \dot{x} &= Ax + Bu + B_d d, \quad \text{with } d = [d_{i1}, d_{i2}]. \\ y &= Cx \end{aligned}$$

We know that $d_{i1} = A_{i1} \sin(4\pi f_c t)$ and $d_{i2} = A_{i2} \sin(6\pi f_c t)$ but we have to determine the magnitudes A_{i1} and A_{i2} . As this disturbance can be considered as an input, we choose to take $B_d = [B \ B]$ and to find the right magnitudes to use.

In order to find A_{i1} and A_{i2} , we evaluate the gain of the transfer function for the three different frequencies. Then, knowing the desired amplitude for each harmonic, we can find the magnitudes A_{i1} and A_{i2} .

```
sys=ss(A,B,C,[0]);
w = [2:2:6]*pi*fc;
[MAG,PHASE] = bode(sys,w)
MAG=[MAG(1) MAG(2) MAG(3)];
[Aifundamental, Ai1, Ai2] = Amplitude(3,1:3)./MAG % = 5.0212    0.0723
0.0792
```

Problem 11

The disturbance is now added to our SIMULINK model (see figure D.1 in Appendix D). The response to the input can be seen figure 1.7 and the PSD figure 1.8.

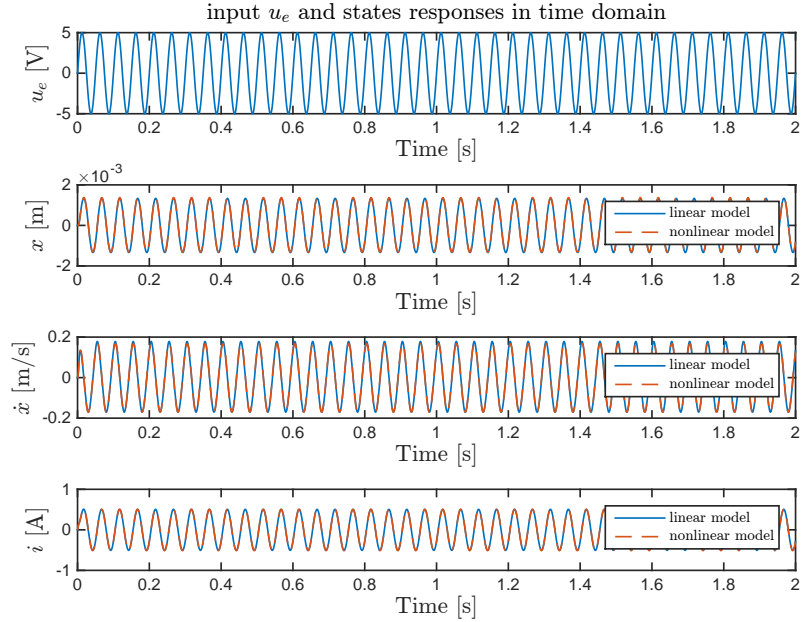


Figure 1.7: response of the states to the input u_e using the linearised model extended with disturbances and the nonlinear model

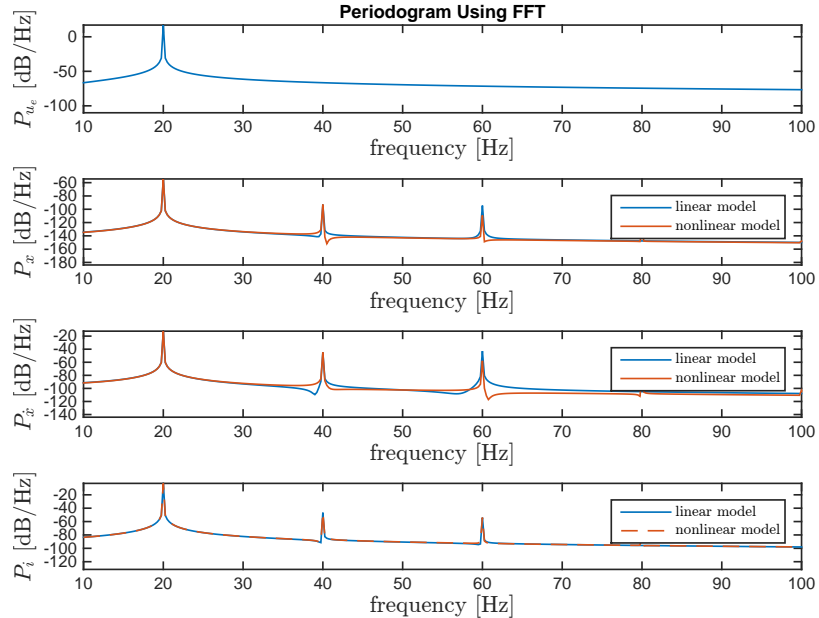


Figure 1.8: PSD of the states using the linearised model extended with disturbances and the nonlinear model

We can see on both figures (1.7 and 1.8) that the responses are almost exactly the same

(the plot of the response of the nonlinear model is over the one of the linear model). As expected, the two harmonic distortions of 40 and 60 Hz are present with the right magnitude. The next distortions are of course missing. Also, the magnitude of the harmonics of state i are almost perfect, but not the ones of the other states which is normal because the disturbance is designed for i .

1.2 Distortion Attenuation

1.2.1 System discretization

Problem 12

We now want to discretize the continuous time linear model. As the smallest constant time is $\tau_2 = 0.0013$ s, we will choose a sampling time $T_s = 0.0001$ s, that is to say 10 times faster. However, this sampling time is the *STEP_SIZE* of the simulation, so the sampling time should be different. Therefore, we will choose $T_s = 0.0002$ s.

Then, we can discretize the linear system using *c2d* MATLAB function.

```
Ts=0.0002; % [s]
[F, G]=c2d(A, B, Ts);
[F, Gd] = c2d(A, Bd, Ts);
lambda=eig(F);
```

The eigenvalues, $\lambda_1 = 0.9426$, $\lambda_2 = 0.8869 + 0.0864i$ and $\lambda_3 = 0.8869 - 0.0864i$, of the discrete time system are inside the unit circle, which means that the system is still asymptotically stable. This result was expected because a discrete time system with a well chosen sampling time is supposed to have the same behavior and be the same system.

Problem 13

The discrete time system was implemented with SIMULINK (see figure E.1 in Appendix E) and simulated with the input $u_e(k) = A_u \sin(2\pi f_c k T_s)$ and the disturbance vector $d(k)$ where $k = [0 \ 1 \ \dots \ \frac{TIME_SIM}{STEP_SIZE} = 50000]$. The results are shown in the time and frequency domains, respectively in figures 1.9 and 1.10 where the responses of P11 are also plotted to allow the comparison.

In the frequency domain (figure 1.10), it can be noticed that the amplitudes of the pikes and their positions in the discrete time model perfectly match the ones in continuous time. The discrete time responses are shifted but that does not impact the system since the amplitudes of the harmonics are the same. Moreover, in the time domain (figure 1.9), the two responses are also similar. For the discrete time system, stairs are visible but since

the time is discretised it is expected. It can then be concluded that the simulation results support the sampling time T_s chosen in P12.

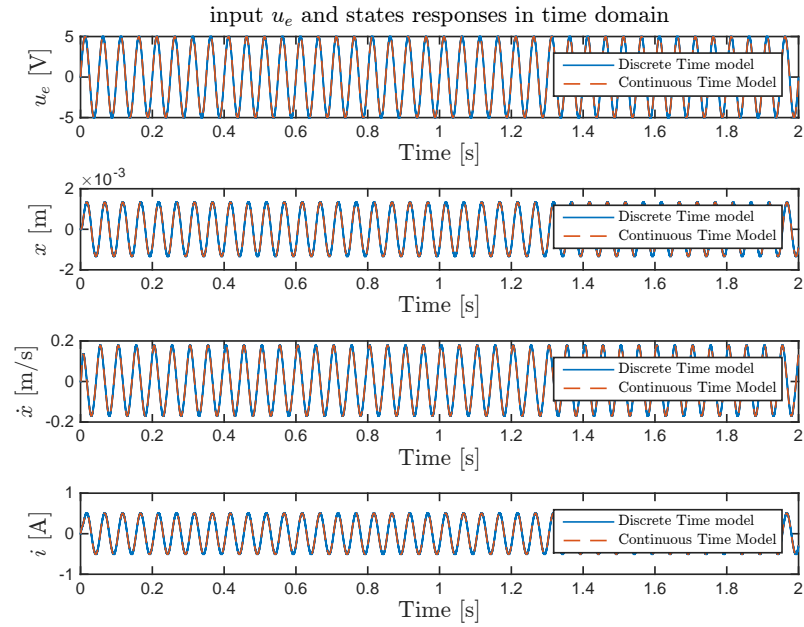


Figure 1.9: Discrete Time Model: input u_e and the states responses in the time domain

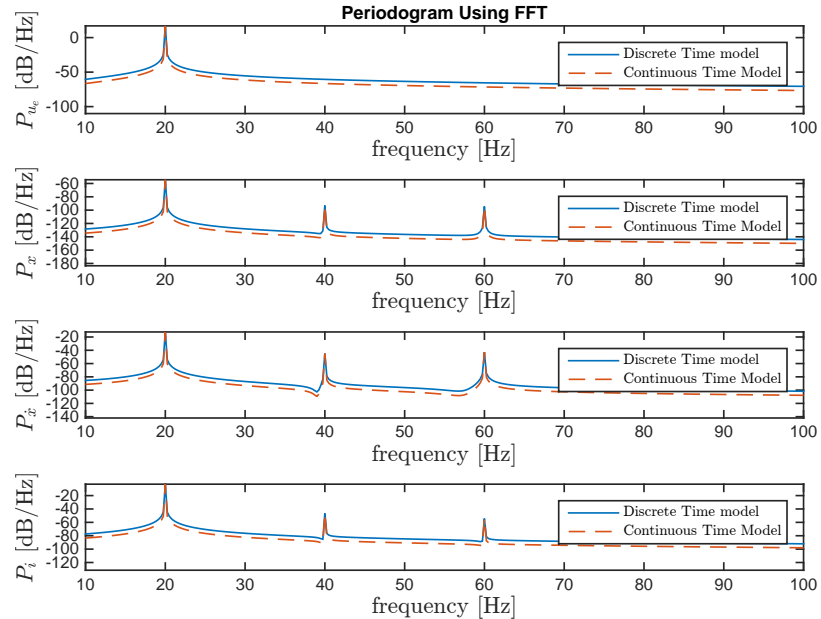


Figure 1.10: Discrete Time Model: input u_e and the states responses in the frequency domain

1.2.2 Voice coil position reference tracking

We would like to reduce the distortion effects by implementing a reference tracking controller for the voice coil position. In order to do so, we consider the same linear model with fictitious disturbances than in P10 and we assume that the state is fully accessible to the measurement. The voice coil position reference $x_{ref}(k) = A_x \sin(2\pi f_c k T_s)$ is given with $A_x \in [0.0005, 0.001]$ m and $f_c \in [20, 200]$ Hz.

Problem 14

The controllability of the system is evaluated numerically by computing the controllability matrix $M_c = [F \ FG \ F^2G]$. The rank of the matrix is equal to 3, which means that the system is controllable: it is possible to achieve the position reference tracking. As the reference signal should not be related to the input signal but directly to the voice coil position, and as it is assumed that the state is measurable, it is proposed to implement a Reference Feedforward Controller. We only want to control x , so the number of control input is equal to the number of controlled output, one in this case.

Problem 15

To design the feedback controller $u_e(k) = \kappa(x(k), x_{ref}(k))$, we want to choose the closed loop eigenvalues by means of the *Arbitrary Eigenvalue Assignment*. According to the control requirement, the frequency band is [20, 200] Hz. The eigenvalues were then selected to have a sharp control between these bounds. To do so, the natural frequency w_n was chosen to be more than $2\pi \cdot 200 = 1.26 \cdot 10^3$ rad/sec. We also wanted a good damping ratio, around 0.7 as well as a fast time constant. Finally the eigenvalues need to have a negative real part to get a stable system. These criteria were fulfilled for the following eigenvalues, converted in discrete time thanks to the formula $\lambda_F = e^{\lambda_A T_s}$:

$$\lambda_{F_{desired}} = \begin{pmatrix} 0.6703 \\ 0.8825 - 0.0885i \\ 0.8825 + 0.0885i \end{pmatrix}$$

As it is explained in P14, the controller to be implemented is a reference feedforward. We have $u_e(k) = -Kx(k) + Nx_{ref}(k)$, where K and N are gains that we need to determine. The feedback gain K is computed thanks to the Ackermann's formula in Matlab $K = acker(F, G, \lambda_{F_{desired}})$ and we obtain our new system with $F_k = F - GK$. The good placement of the eigenvalues is checked thanks to the *eig* function. The bode diagram is also plotted (figure 1.11) and it can be verified that the gain is constant for the frequency band desired from 20 to 200 Hz i.e. from 126 rad/sec to $1.26 \cdot 10^3$ rad/sec. At 200 Hz, the

gain is slowly decreasing but in order to have a control input in the range -40 and 40 V, we have to find a trade-off and it was chosen not to track perfectly the reference for 200 Hz instead of having a saturated input.

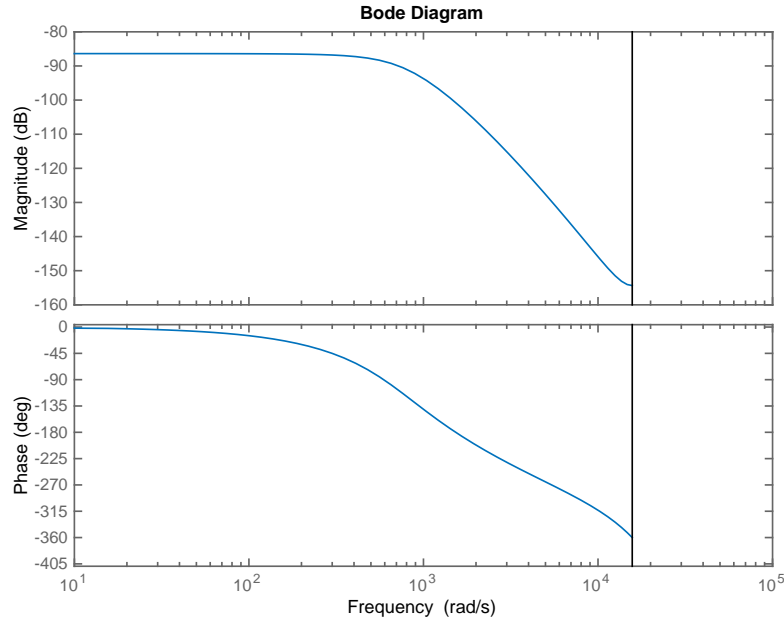


Figure 1.11: Bode Diagram of the Discrete Time System with Feedback Controller

Once this step achieved, we compute N (1.24) through the DC gain κ of the closed-loop system (1.23):

$$\kappa = C(I - F_k)^{-1}G \quad (1.23)$$

$$N = \kappa^{-1} \quad (1.24)$$

After implementing the controller in Simulink (see Appendix F), the simulation was run. It can be noticed on figure 1.12 that the voice coil position matches well the reference x_{ref} with a time delay $\tau = 4 \text{ ms}$.

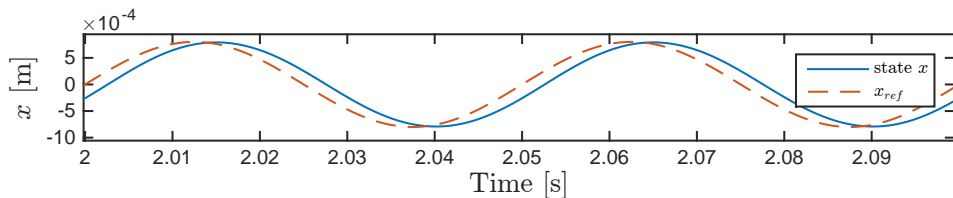


Figure 1.12: Simulation of the Discrete Time Linear Model with the Position Reference Tracking

Problem 16

In order to test the performance of the discrete controller, it has been implemented on the continuous time linear system (SIMULINK model figure G.1 in Appendix G).

As we can see figure 1.13 and figure 1.14, the controller works well, that is to say, the reference position is well followed. Indeed, with or without the noise \mathbf{d} , the tracking is the same, with a delay $\tau = 0.0026$ s

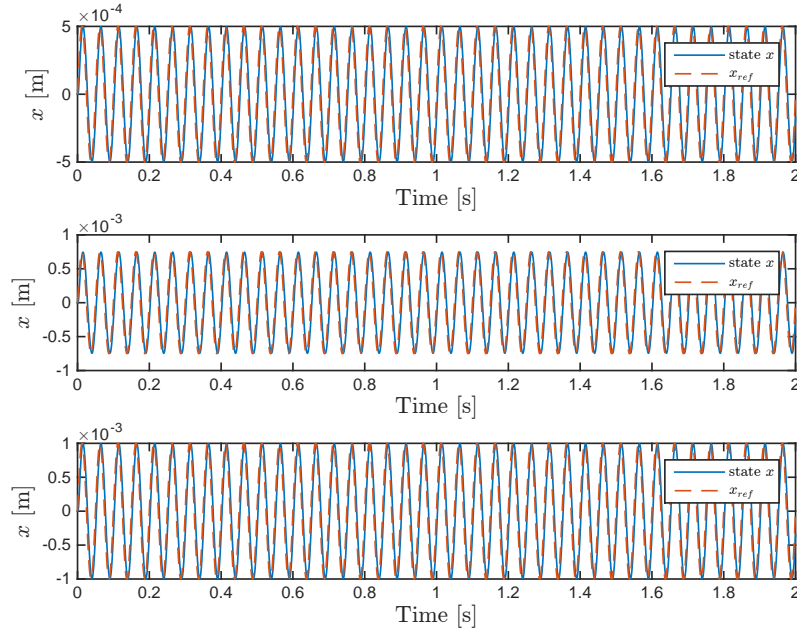


Figure 1.13: response of the state x to the input x_{ref} with $Ax = [0.0005, 0.00075, 0.001]$ (from the top to the bottom) with the controller without noise

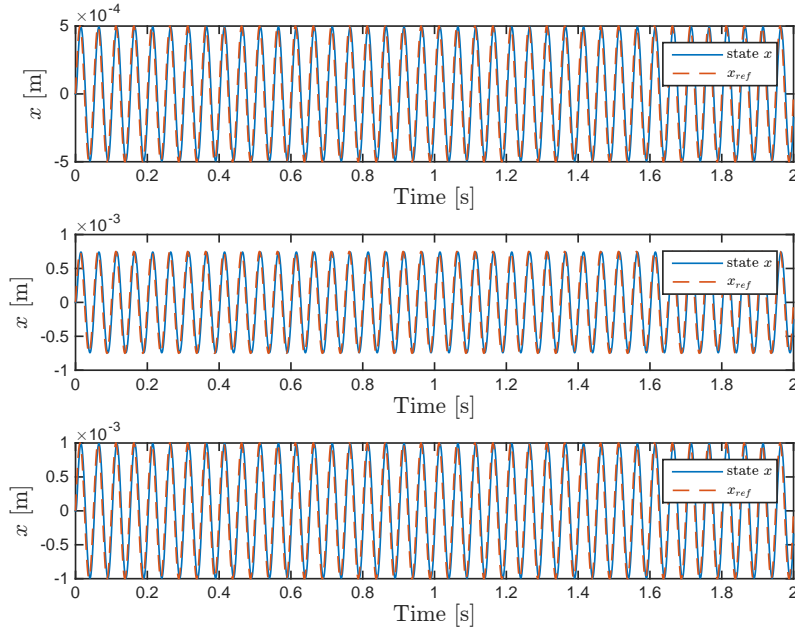


Figure 1.14: response of the state x to the input x_{ref} with $Ax = [0.0005, 0.00075, 0.001]$ (from the top to the bottom) with the controller with the noise \mathbf{d}

We can notice that it is odd that there is no difference between the simulation with or without the noise \mathbf{d} .

Problem 17

In this problem, the discrete time feedback is tested on the nonlinear model. The controller has been implemented on the SIMULINK model of the nonlinear system (see figure H.1 in Appendix H).

The state responses to x_{ref} has been plotted figure 1.15 in the time domain and figure 1.16 in the frequency domain.

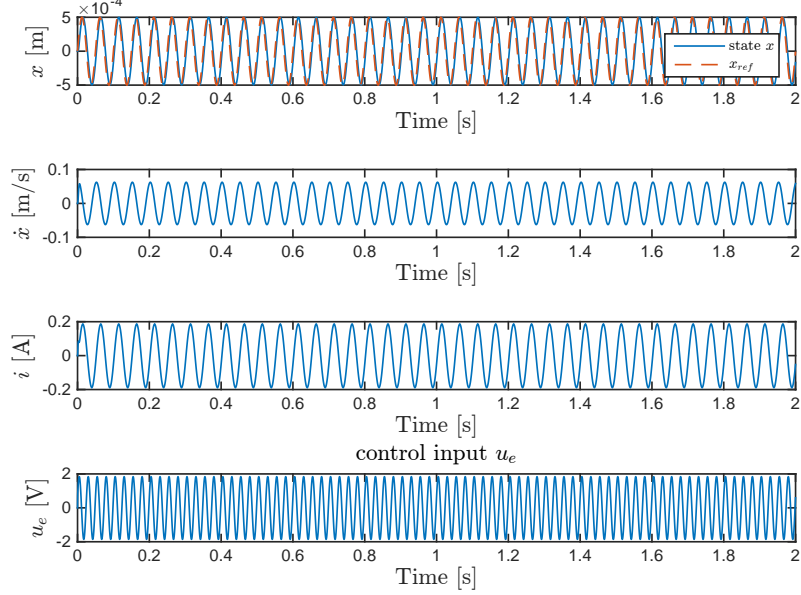


Figure 1.15: u_e and state responses to x_{ref} with $Ax = 0.0005$ m using the controller on the nonlinear model.

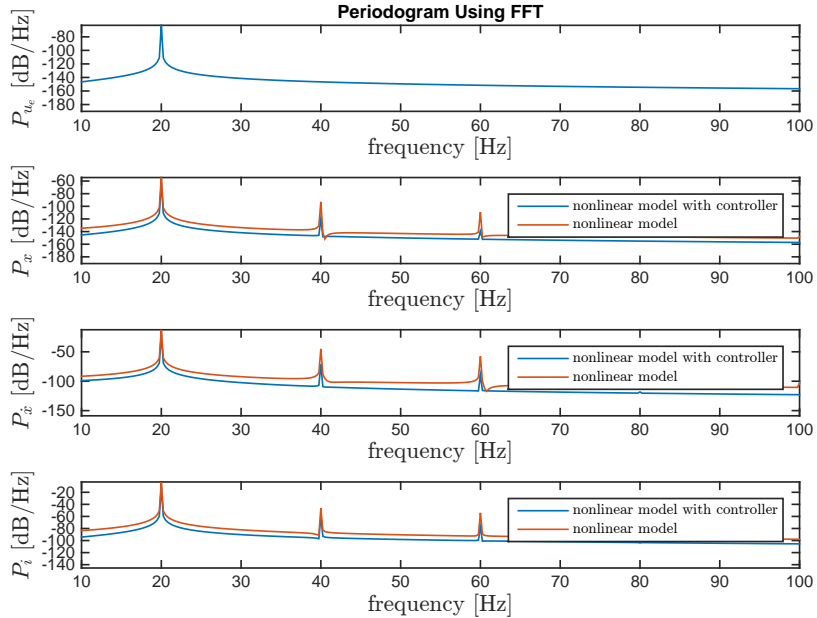


Figure 1.16: PSD of u_e and the states response to x_{ref} with $Ax = 0.0005$ m using the controller on the nonlinear model.

As we can see figure 1.15, the reference is well tracked with a delay $\tau = 0.0034$ s. Moreover, u_e has also been plotted figure 1.15 and we can notice that $\max(u_e) \simeq 2 < 5$ V, which respects the condition of the maximum voltage. The simulation has also been run with $Ax = 0.001$ m and $\max(u_e) \simeq 3.7 < 5$ V too.

Also, we can see figure 1.16 that the harmonic distortion is attenuated. Indeed, we can

see tab 1.17 that the percentage of the *Total Harmonic Distortion (THD)* has decreased a lot, there is only 12% of the initial THD left. Moreover, the distortion level of the second and third harmonic (d_2, d_3) have decreased a lot too (13 and 7% left). Therefore, we can say that the controller succeeded in attenuating the harmonic distortion.

	with controller	without controller
THD	0.3029 %	2.4350 %
d_2	0.3005 %	2.3735 %
d_3	0.0383 %	0.5432 %

Figure 1.17: THD, d_2 an d_3 of the coil velocity with the nonlinear model with and without controller (include the first 5 harmonics after the fundamental frequency $f_c = 20 \text{ Hz}$)

Problem 18

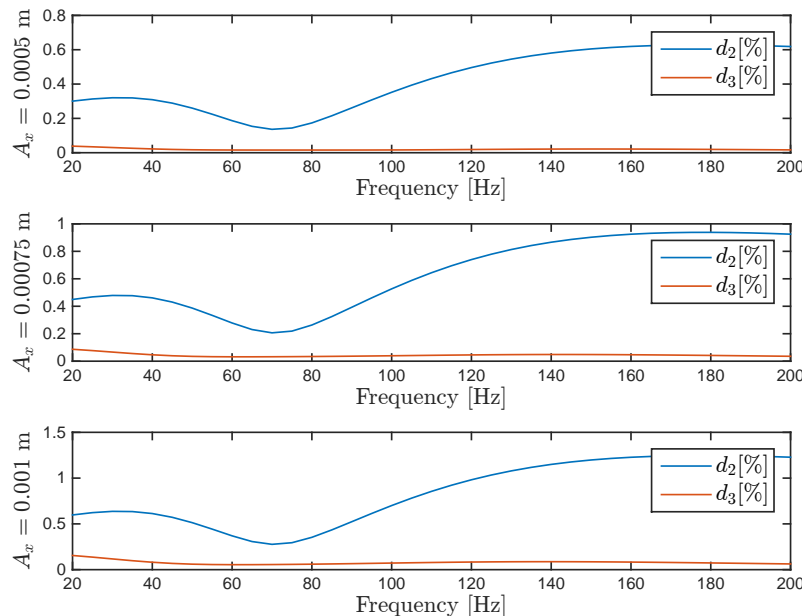


Figure 1.18: Effect of the variations of the frequency f_c and the amplitude A_x of the voice coil position x_{ref} on the second and third order harmonic distortion

In order to study the effect of the variations of the frequency f_c and the amplitude A_x of the voice coil position x_{ref} on the second and third order harmonic distortions, we have computed d_2 and d_3 for a range of A_x and f_c . The results can be seen on the figure 1.18. According to the graphic, the variations of the amplitude of the reference do not affect the shape of the distortion levels but their pourcentage, as it was the case in P5. On the other hand, in P5 the distortions levels were higher for 20 Hz than 200 Hz. It is the contrary in P18. That can be explained by the choice of the eigenvalues of the closed loop system. The controller is less effective around 200 Hz, that why the distortion levels are less attenuated. Finally we can notice that compared to P5, d_2 and d_3 have lower values

and are close to 0%, especially d_3 , which shows that the designed controller accomplishes its task, that is to say reducing the distortion effects.

1.2.3 Output feedback voice coil position tracking control with disturbance rejection

To attenuate the distortion around the second and third order harmonics, an observer will be implemented in the linear system to approximate the fictitious disturbances and deduce the behaviour of the nonlinear system. We still have $y(t) = i(t)$ and the model described below is considered:

$$\dot{x} = Ax + Bu_e + B_d d$$

$$y = Cx$$

where $C = [0 \ 0 \ 1]$. The voice coil position reference $x_{ref}(k) = A_x \sin(2\pi f_c k T_s)$ with $A_x = 0.001$ m and $f_c = 20$ Hz is given.

Problem 19

In order to recreate the fictitious disturbances and the unmeasured states, the model is expanded with 4 new states. The new model is:

$$\dot{x}_k = A_k x_k + B_k u_e + B_{kn} n_1$$

$$y = C_k x_k + n_2$$

where A_k , B_k , B_{kn} and C_k need to be determined. To do so, the dynamics of the disturbance d is designed with a new system such as:

$$\dot{w} = A_w w$$

$$d = C_w w$$

Where $Re(\lambda(A_w)) = 0$. This means that the eigenvalues of each disturbance should be on the imaginary axes and be conjugate pairs. As a reminder, we also have:

$$d = \begin{pmatrix} \sin(4\pi f_c t) \\ \sin(6\pi f_c t) \end{pmatrix}$$

The disturbance d is composed of two sinusoidal signals (sinus). In Laplace domain, their poles will be on the imaginary axes, at $\pm j\omega$ where $\omega = 4\pi f_c$ for d_1 and $\omega = 6\pi f_c$ for d_2 , which is desired. The transfert functions corresponding to each disturbance using the

Matlab *laplace* function are calculated:

$$H_1(s) = \frac{80\pi}{s^2 + 6400\pi^2}$$

$$H_2(s) = \frac{120\pi}{s^2 + 14400\pi^2}$$

Then we use *tf2ss* to have the two subsystems ($A_{w_1}, B_{w_1}, C_{w_1}$ and D_{w_1} and $A_{w_2}, B_{w_2}, C_{w_2}$ and D_{w_2}) corresponding to each transfert function. A_w and $A_{xw} = B_d C_w$ are deduced by combining the two subsystems:

$$A_w = \begin{pmatrix} 0 & -6.3165 \cdot 10^4 & 0 & 0 \\ 1 & 0 & 0 & 0 \\ 0 & 0 & 0 & -1.4212 \cdot 10^5 \\ 0 & 0 & 1 & 0 \end{pmatrix} \quad A_{xw} = \begin{pmatrix} 0 & 0 & 0 & 0 \\ 0 & 0 & 0 & 0 \\ 0 & 4.4483 \cdot 10^4 & 0 & 6.6724 \cdot 10^4 \end{pmatrix}$$

And finally:

$$A_k = \begin{pmatrix} A & A_{xw} \\ 0_{4 \times 3} & A_w \end{pmatrix} \quad B_k = \begin{pmatrix} B \\ 0_{4 \times 1} \end{pmatrix} \quad C_k = \begin{pmatrix} C & 0_{1 \times 4} \end{pmatrix}$$

As the process noise n_x enters the system in the feedback path of the open loop system, it is multiplied by the matrix A ($A_k(x_k + n_x) = A_k x_k + A_k n_x$). Thus, a part of the matrix A moves into B_{kn} . Then we have:

$$B_{kn} = \begin{pmatrix} A_{bis} & 0_{3 \times 4} \\ 0_{4 \times 3} & Id_4 \end{pmatrix} \quad A_{bis} = \begin{pmatrix} 0 & 0 \\ 0 & A(2,2) \\ A(3,3) & 0 \end{pmatrix}$$

Problem 20

In order to include the proper noise models, we augment the system of Problem 19 with n_x . Thus, our new state vector is $x_a = (i, x, \dot{x}, x_{d1}, x_{d2}, x_{d3}, x_{d4}, n_i, n_v)^T$. As n_x is a band-limited noise characterized by $R(\tau) = \sigma^2 e^{-\beta|\tau|}$, we have $n_x = A_{nx} n_x + B_{nx} w$ with

$$A_{nx} = \begin{pmatrix} -\beta & 0 \\ 0 & -\beta \end{pmatrix} \quad B_{bn} = \begin{pmatrix} \sqrt{2\beta} \sigma_{nx1} & 0 \\ 0 & \sqrt{2\beta} \sigma_{nx2} \end{pmatrix} \quad w = \begin{pmatrix} w_1 \\ w_2 \end{pmatrix}$$

Thus, our new process noise v is $(n_{d1}, n_{d2}, n_{d3}, n_{d4}, w_1, w_2)^T$ and the system is :

$$\dot{x}_a = A_a x_a + B_a u_e + B_{av} v$$

$$y = C_a x_a + n_2 \quad \text{with } C_a = \begin{pmatrix} C_{kn} & 0_{1 \times 2} \end{pmatrix}$$

$$A_a = \begin{pmatrix} A_k & B_{knbis} \\ 0_{2 \times 1} & A_{nx} \end{pmatrix} \quad B_a = \begin{pmatrix} B_k \\ 0_{4 \times 1} \end{pmatrix} \quad B_{av} = \begin{pmatrix} 0_{3 \times 6} & 0_{1 \times 2} \\ V_{nd} & 0_{1 \times 2} \\ 0_{2 \times 1} & B_{nx} \end{pmatrix} \quad B_{knbis} = \begin{pmatrix} A_{bis} \\ 0_{2 \times 2} \end{pmatrix}$$

Problem 21

In order to design a discrete time Kalman filter for the previous model, the first step is to discretize the covariance matrix V_{nd} . As the smallest constant time of the system is bigger than the T_s , we can discretize it as following.

```
Vnwdisc = Bva * [Vnd zeros(4,2); zeros(2,4) diag([sigmai sigmav])] * Bva' * Ts;
sigman2d = sigman2/Ts;
[M, P, Z, E] = dlqe(Fa, Gva, Ca, Vnwdisc, sigman2d);
```

However, the *dlqe* function of MATLAB does not accept our these matrices because V_{nwdisc} must be square with as many columns as G_{va} .

Problem 22

Even if the matrix M of the Kalman filter has not been found, the SIMULINK model has been implemented (see Appendix I).

Appendix A

SIMULINK Model of the Nonlinear System

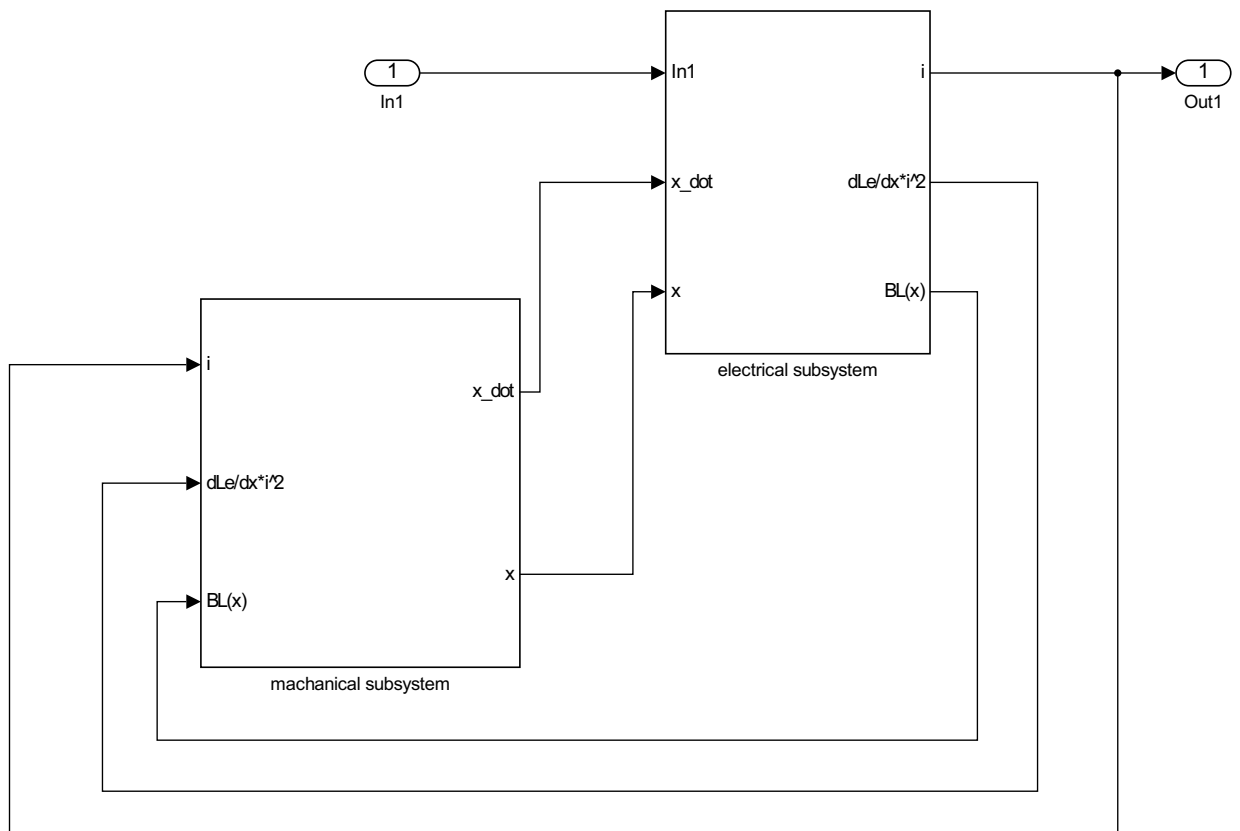


Figure A.1: SIMULINK Model of the Nonlinear System

Appendix B

Block Diagram of the Linearised Loudspeaker

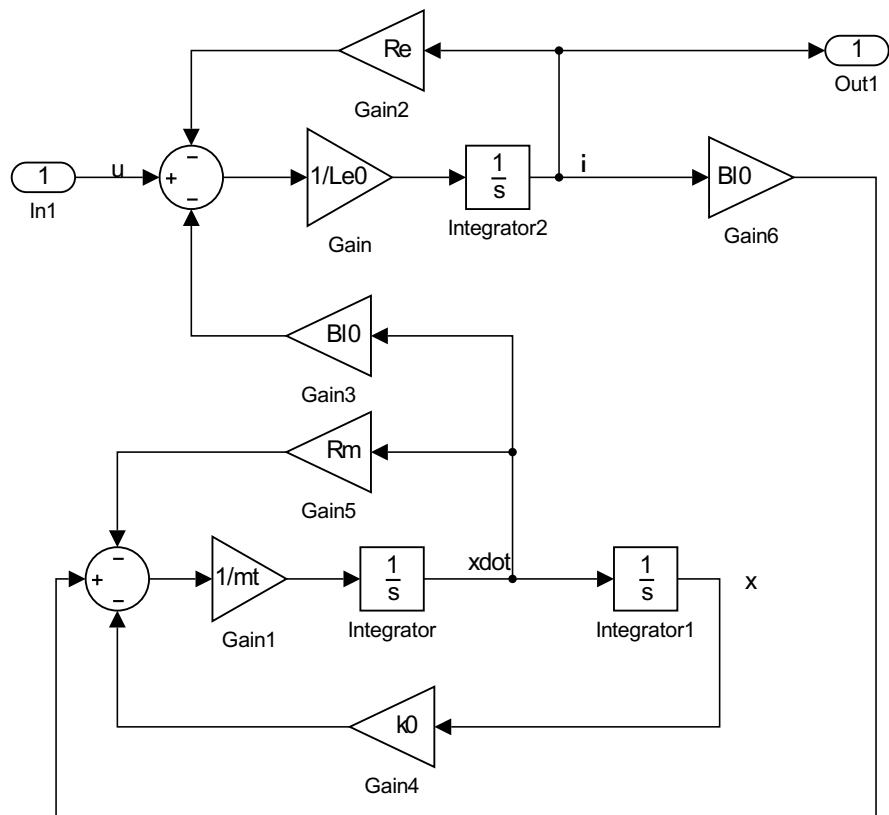


Figure B.1: Block diagram of the linearised loudspeaker

Appendix C

SIMULINK Model of the Linear System

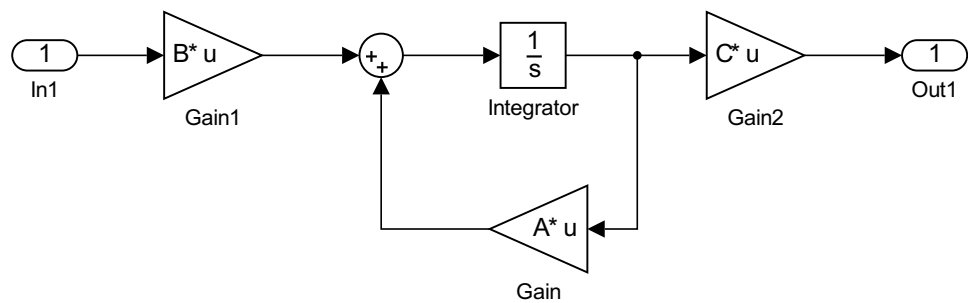


Figure C.1: SIMULINK model of the linearised loudspeaker

Appendix D

SIMULINK Model of the Linear System with Disturbance in Continuous Time

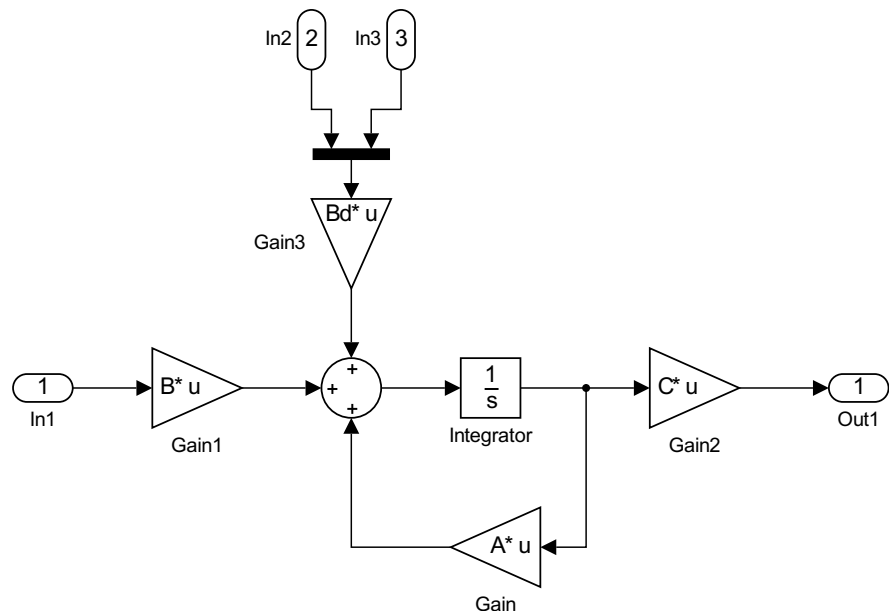


Figure D.1: SIMULINK model of the linearised loudspeaker with noise

Appendix E

SIMULINK Model of the Linear System with Disturbance in Discrete Time

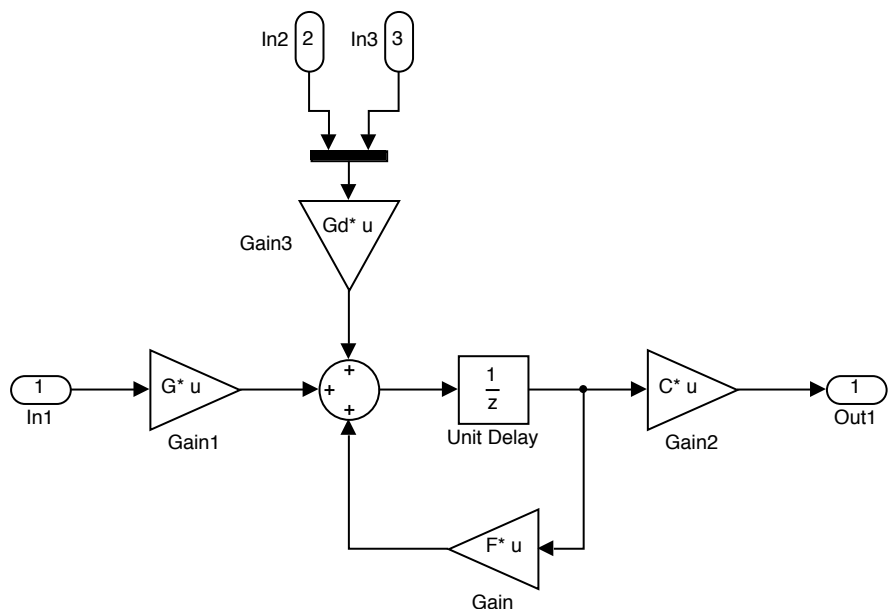


Figure E.1: SIMULINK Model of the Linear System with Disturbance in Discrete Time

Appendix F

SIMULINK Model of the Discrete Time Linear System with the Feedback Controller

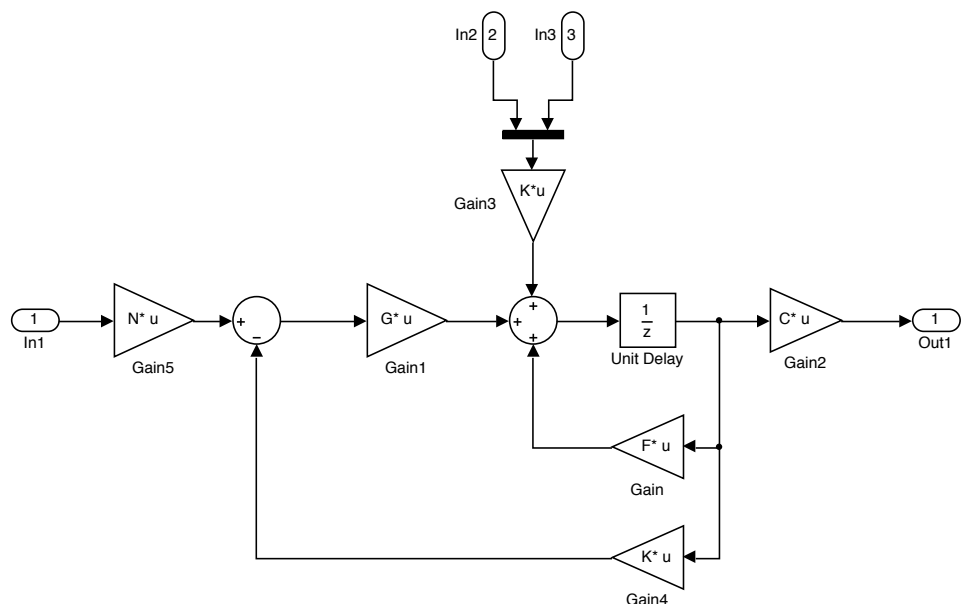


Figure F.1: SIMULINK Model of the Discrete Time Linear System with the Feedback Controller

Appendix G

SIMULINK Model of the Continuous Time Linear System with the Discrete Time Feedback

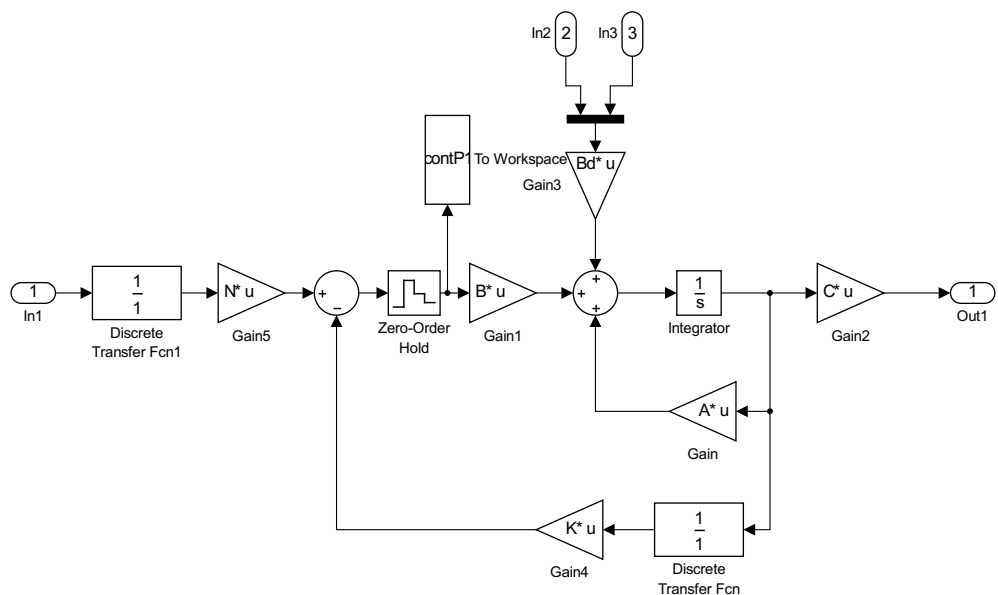


Figure G.1: SIMULINK Model of the Continuous Time Linear System with the Discrete Time Feedback

Appendix H

SIMULINK Model of the Nonlinear Model with the Discrete Time Feedback

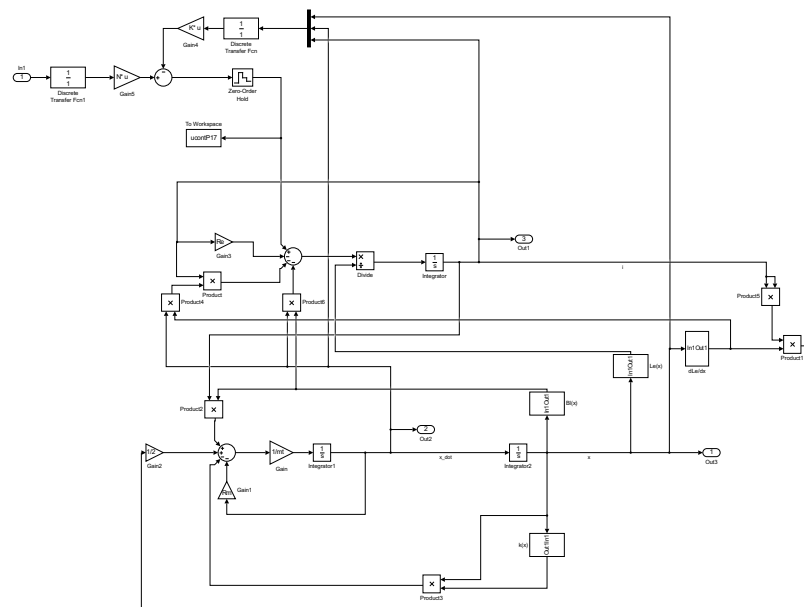


Figure H.1: SIMULINK Model of the Nonlinear Model with the Discrete Time Feedback

Appendix I

SIMULINK Model of Kalman filter for the linear model with disturbance

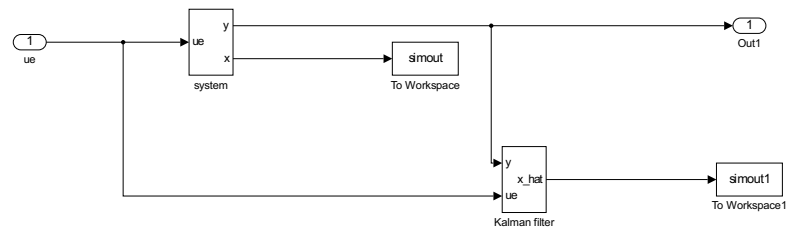


Figure I.1: SIMULINK Model of the system with the Kalman filter

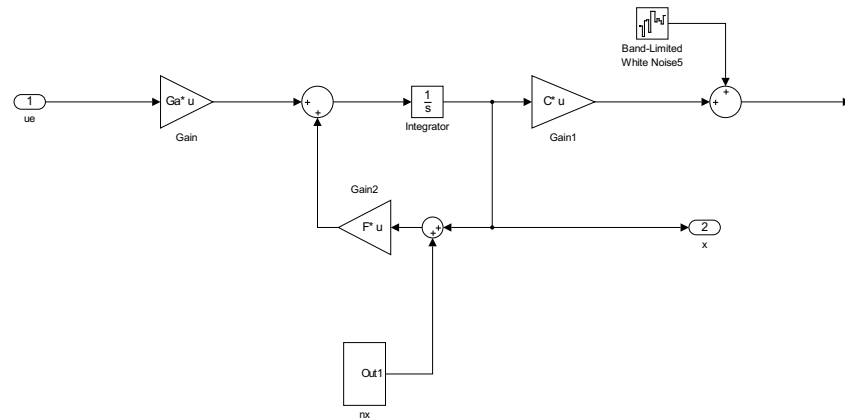


Figure I.2: SIMULINK Model of the linear model with process noise

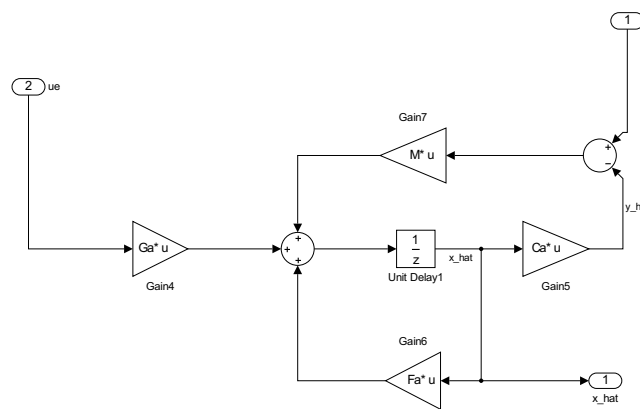


Figure I.3: SIMULINK Model of Kalman filter

Bibliography

- [1] Roberto Galeazzi, *Manual For Compulsory Exercise*, 2015.